

Published in final edited form as:

J Cataract Refract Surg. 2013 January ; 39(1): 110–117. doi:10.1016/j.jcrs.2012.07.040.

Quality of corneal lamellar cuts quantified using atomic force microscopy

Noël M. Ziebarth, PhD, Janice Dias, BS, Volkan Hürmeriç, MD, Mohamed Abou Shousha, MD, Chiyat Ben Yau, PhD, Vincent T. Moy, PhD, William Culbertson, MD, and Sonia H. Yoo, MD

Biomedical Atomic Force Microscopy Laboratory (Ziebarth, Dias), Department of Biomedical Engineering, University of Miami College of Engineering, Coral Gables, and the Bascom Palmer Eye Institute (Hürmeriç, Shousha, Culbertson, Yoo) and the Department of Physiology and Biophysics (Yoo, Moy), University of Miami Miller School of Medicine, Miami, Florida, USA

Abstract

PURPOSE—To quantify the cut quality of lamellar dissections made with the femtosecond laser using atomic force microscopy (AFM).

SETTING—Bascom Palmer Eye Institute, University of Miami Miller School of Medicine, Miami, Florida, USA.

DESIGN—Experimental study.

METHODS—Experiments were performed on 3 pairs of human cadaver eyes. The cornea was thinned to physiologic levels by placing the globe, cornea side down, in 25% dextran for 24 hours. The eyes were reinflated to normal pressures by injecting a balanced salt solution into the vitreous cavity. The eyes were placed in a holder, the epithelium was removed, and the eyes were cut with a Visumax femtosecond laser. The energy level was 180 nJ for the right eye and 340 nJ for the left eye of each pair. The cut depths were 200 μm , 300 μm , and 400 μm , with the cut depth maintained for both eyes of each pair. A 12.0 mm trephination was then performed. The anterior portion of the lamellar surface was placed in a balanced salt solution and imaged with AFM. As a control, the posterior surface was placed in 2% formalin and imaged with environmental scanning electron microscopy (SEM). Four quantitative parameters (root-mean-square deviation, average deviation, skewness, kurtosis) were calculated from the AFM images.

RESULTS—From AFM, the 300 μm low-energy cuts were the smoothest. Similar results were seen qualitatively in the environmental SEM images.

© 2012 American Society of Cataract and Refractive Surgery and European Society of Cataract and Refractive Surgeons. Published by Elsevier Inc. All rights reserved.

Corresponding author: Noël M. Ziebarth, PhD, University of Miami, Department of Biomedical Engineering, McArthur Annex Room 209, 1251 Memorial Drive, Coral Gables, Florida 33146, USA. nziebarth@miami.edu.
Jorge Peña, MD, Florida Lions Eye Bank, donated the human eyes.

Publisher's Disclaimer: This is a PDF file of an unedited manuscript that has been accepted for publication. As a service to our customers we are providing this early version of the manuscript. The manuscript will undergo copyediting, typesetting, and review of the resulting proof before it is published in its final citable form. Please note that during the production process errors may be discovered which could affect the content, and all legal disclaimers that apply to the journal pertain.

Financial Disclosure: No author has a financial or proprietary interest in any material or method mentioned.

Presented in part at the annual meeting of the Association for Research in Vision and Ophthalmology, Fort Lauderdale, Florida, USA, May 2010, and the VI World Cornea Congress, Boston, Massachusetts, USA, April 2010.

Cadaver corneas were sectioned at 3 depths with 2 energy levels using a femtosecond laser. The 300 μm low-energy cuts were the smoothest.

CONCLUSION—Atomic force microscopy provided quantitative information on the quality of lamellar dissections made using a femtosecond laser, which is useful in optimizing patient outcomes in refractive and lamellar keratoplasty surgeries.

The femtosecond laser is gaining popularity in the corneal refractive surgery arena, and multiple systems have been approved by the U.S. Food and Drug Administration to create the flap during laser in situ keratomileusis (LASIK). This laser is also being used in lieu of traditional trephines for penetrating keratoplasty procedures. In addition, the femtosecond laser is being used to prepare donor and recipient corneas for anterior lamellar keratoplasty (ALK)¹ and Descemet-stripping automated endothelial keratoplasty (DSAEK) procedures. In LASIK and lamellar transplant surgeries (DSAEK and ALK), a smooth stromal surface will create a clearer interface, which in turn will produce better optical quality.² Therefore, it is vital to quantitatively analyze the stromal cut quality produced using different lasers and settings as well as at different depths in the stroma.

Several studies have assessed stromal smoothness after cutting with different femtosecond lasers to evaluate their efficacy. The smoothness of the stromal bed after performing LASIK flaps and deep lamellar cuts (~400 μm) has been studied by several research groups using scanning electron microscopy (SEM).²⁻¹² The smoothness of the cuts was determined qualitatively by visual inspection because SEM images alone cannot provide quantitative roughness information. However, using Scanning Probe Image Processor software (Image Metrology) to analyze the SEM images, quantitative surface roughness can be extracted.^{8,9} This software produces a 3-dimensional (3-D) reconstruction of the sample surface based on differences in darkness of the grayscale images. To more accurately assess the smoothness of the stromal bed, however, it is vital to use a technique that provides numerical data of the surface topography. A profilometer based on the principle of 3-D confocal microscopy has been applied to the stromal surface to provide quantitative roughness information.¹¹ Atomic force microscopy (AFM) has also been used to image the corneal surface quality after photorefractive keratectomy^{13,14} and to quantify the smoothness of femtosecond laser cuts made in the posterior cornea at different laser energies.¹⁵ Atomic force microscopy was first developed by Binnig et al.¹⁶ as a tool to investigate the topography of conductors and insulators on the atomic scale. It was rapidly improved to enable operation in liquids, which made characterization of biological samples possible. Atomic force microscopy uses a sharp tip at the end of a flexible cantilever to scan and probe the sample surface. A force on the order of piconewtons is created on the cantilever due to the proximity to the sample surface. This force is kept constant with a feedback mechanism that raises and lowers the cantilever by means of a piezoelectric element. By keeping the force constant, the tip remains at the same distance from the surface of the sample and thereby maps out the surface topography.^{16,17} Atomic force microscopy can achieve resolutions of 0.1 Å and has the ability to measure immersed samples.

The purpose of the current study was to build on previous corneal smoothness studies¹⁵ and use AFM to quantify the cut quality of lamellar dissections made with a femtosecond laser (Visumax, Carl Zeiss Meditec AG) at 2 laser energy settings and 3 distinct depths in the corneal stroma.

MATERIALS AND METHODS

Experimental Protocol

Experiments were performed on pairs of human eyes obtained from the Florida Lions Eye Bank, Miami, Florida. Human eyes were obtained and used in compliance with the guidelines of the Declaration of Helsinki for research involving the use of human tissue. The eyes obtained from the eye bank had been deemed unsuitable for corneal transplantation;

thus, they had not been placed in storage medium immediately after death. Because of this, the corneal endothelial cells were no longer viable and the corneas showed a considerable degree of edema.

To restore the corneal thickness and hydration to physiologic levels, the eyes were placed cornea side down in 25% dextran on arrival in the laboratory.¹⁸ The globes were stored in dextran overnight in the refrigerator at 4°C. Before experimentation, the globes were injected with a balanced salt solution (BSS, Alcon Laboratories, Inc.) in the vitreous cavity until the intraocular pressure was increased to approximately 15 mm Hg. The epithelium was then removed using alcohol and a #69 Beaver blade. The whole globe was placed in a purpose-designed holder under the femtosecond laser (500 kHz), and the cutting was performed. Table 1 shows the cut energy and the cut depth. The cut depth was maintained in the right eye and left eye of each pair. In all eyes, the lamellar cut diameter was 7.0 mm, the lamellar spot and line separations were 1.6 μm , and the lamellar cut method was performed in a spiral pattern beginning from the corneal center. The line separation for the LASIK flaps and the 2 energy levels were based on the low and the high ends of what is typically used clinically with the femtosecond laser to create LASIK flaps. All globes were imaged with an optical coherence tomography (OCT) system (Visante, Carl Zeiss Meditec AG) to verify the depth of the cut. When complete, a 12.0 mm trephination of the cornea was performed. The stromal surface of the anterior corneal lenticule of the sectioned cornea was placed in a balanced salt solution and transported for imaging with the AFM. Imaging with the AFM began less than 2 hours after sectioning with the femtosecond laser. The posterior face of the lamellar incision was placed in 2% formalin and transported for imaging with an environmental SEM to serve as a control.

Atomic Force Microscope Imaging

A commercial atomic force microscope (MFP-3D-BIO, Asylum Research) was used to obtain high-magnification images of the cornea sectioned with the femtosecond laser. Care was taken to ensure that the cut surface was oriented upward before imaging began. This was verified by placing the cornea so that its natural curvature formed a bowl when placed on the glass slide. Because this curvature interferes with the cantilever contact with the sample, 4 slits were made around the periphery of the cornea so that it would remain flat on the glass slide. The images were obtained in contact mode, in which the cantilever tip is kept in continuous contact with the sample surface, maintaining constant cantilever deflection while scanning. The piezoelectric mechanism applies vertical position corrections to keep this deflection constant, thereby mapping the actual 3-D topography of the sample surface. Peak-to-peak heights up to 15 μm can be distinguished in this mode. Although tapping-mode imaging has lower lateral drag forces that may damage the sample, contact mode was selected because the lateral forces present on compliant samples during tapping mode will likely blur the surface features that are important in roughness analysis. A pyramidal, silicon nitride AFM cantilever tip (40 nm tip diameter, nominal spring constant 0.01 N/m, MLCT series, Bruker AFM Probes) was used to image all samples. Each sample was imaged in 3 discrete spots across the surface with scan sizes of 10 $\mu\text{m} \pm 10 \mu\text{m}$, 50 $\mu\text{m} \pm 50 \mu\text{m}$, and 90 $\mu\text{m} \pm 90 \mu\text{m}$ in each spot (total of 9 images per sample). All images were acquired with a 512 point \pm 512 point resolution. Hydration of the samples was maintained throughout the experiments by placing drops of a balanced salt solution on the exposed surface.

Data and Statistical Analysis

All images of the corneal samples were analyzed with the MFP3D program (Igor Pro, Wavemetrics, Inc.) included with the atomic force microscope. To compensate for differences in the starting height of the piezoelectric actuator and in the sample slant, the background slope was removed from all images.¹⁵ The following 4 quantitative parameters

were used to characterize the roughness of the corneal stromal surface: root-mean-square (RMS) deviation, average deviation, skewness (asymmetry around the mean), and kurtosis (peakedness or flatness compared with the average height). These values were calculated from each height image using the MFP3D program. Any images with motion or adhesion artifacts were excluded from the analysis.

Statistical analysis used 2-factor (depth, energy level) analysis of variance (ANOVA) followed by post hoc least significant difference tests, as appropriate. In the event of an interaction between the 2 factors, 1-way ANOVA and 2-sample *t* tests were used to assess differences within each energy level and within each cut depth.

The images obtained with the environmental SEM were compared, and the roughness was scaled relatively between samples. These relative results were then compared with the AFM quantitative measurements.

RESULTS

Experiments were performed on 3 pairs of human eyes (Table 1).

Figures 1 to 3 show representative height and deflection images obtained using AFM. These images represent the raw data outputted directly from the image acquisition program included with the atomic force microscope. The height image gives the exact vertical displacement of the cantilever tip as it scanned up and down across the topography of the sample. This image was analyzed to provide the roughness information. The deflection image provides the degree of bending of the cantilever as it scans across the sample. This image gives an indication of the hardness of the sample. Typically, the deflection image provides a more detailed view of the sample ultrastructure. When imaging, the AFM produces a trace and retrace image in the same area of the sample. The retrace images did not have noticeable artifacts that could have been due to cantilever contact.

Table 2 shows the roughness parameters for the 6 human eyes. The 2-factor ANOVA of the RMS, average deviation, and skewness data identified a significant interaction between energy and depth ($P = .069$, $P = .063$, and $P = 0.064$, respectively). Therefore, it cannot be assumed that the difference between depths was similar for both low energy and high energy. Thus, the differences between the 3 depths in each energy level were independently analyzed from the low energy versus high energy for each cut depth. Analysis of the RMS data showed that the low-energy cut was significantly smoother than the high-energy cut for the 300 μm depth only. The average deviation data showed a significant difference between cut depths for low energy only, with the 300 μm cut having a smaller average deviation than the 200 μm cut ($P = .015$). At the low energy, the 200 μm and 300 μm cuts had comparable skewness ($P = .357$), which was significantly less than that for the 400 μm cuts ($P = .029$). Because higher the kurtosis values mean rougher samples, the kurtosis data suggest that the 400 μm cut was significantly rougher than the 200 μm cut ($P = .002$) and the 300 μm cut ($P = .039$). Therefore, in summary, the results suggest that the 300 μm low-energy cut had the smoothest surface.

Figure 4 shows the images obtained with the environmental SEM on the posterior face of the lamellar incision of same samples used for the AFM imaging studies. Qualitatively, the cuts at 300 μm appeared the smoothest, followed by the 200 μm cuts and then the 400 μm cuts. These results corresponded to the quantitative AFM data and the statistical analysis of the data. The low-energy and high-energy cuts appeared to have similar smoothness based on the environmental SEM images.

DISCUSSION

In this pilot study, human cadaver corneas were sectioned at 3 distinct depths with 2 energy settings using the Visumax femtosecond laser. Atomic force microscopy was used to provide quantitative information on the cut smoothness. The samples were imaged immediately after cutting, and hydration was maintained throughout the imaging. Four quantitative roughness parameters calculated directly from AFM measurements were used to quantify cut smoothness. The roughness was calculated from the actual vertical adjustments made by the piezoelectric mechanism as it scanned across the sample. The vertical range of the piezoelectric mechanism allows roughness measurements up to 15 μm with subnanometer precision.

As a control, the samples were imaged with an environmental SEM. The smoothness of the cuts at each depth was qualitatively graded relative to each other, and it was determined that the 300 μm cuts were the smoothest, as was determined from the quantitative AFM results. However, simple inspection of the environmental SEM images was insufficient to make conclusions about relative differences between low energy and high energy. The quantitative AFM results showed that the low-energy cuts were smoother than high-energy cuts at a depth of 300 μm in the cornea.

Because the smoothness of the lamellar section affects visual and refractive outcomes of the patient,⁷⁻¹⁰ it is important to carefully select the laser settings to optimize postoperative quality of vision. In this study, we compared 2 laser energies; that is, 180 nJ (low) and 340 nJ (high). Using the Visumax femtosecond laser, the low-energy cuts were smoother at a depth of 300 μm in the cornea, although no statistically significant relationship was found for low-energy versus high-energy cuts at 200 μm and 400 μm . A recent study by Serrao et al.¹⁵ evaluated the smoothness of the corneal stroma after sectioning with the Intralase iFS femtosecond laser (Advanced Medical Optics, Inc.) with different laser settings by imaging with AFM. They found that roughness increased with increasing laser power. Although their study found the same qualitative results as the current study, the quantitative values reported by Serrao et al. for RMS roughness and average deviation were approximately 5 times smaller, although the image analysis protocol was the same. The difference is most likely the result of the methodology; that is, the femtosecond laser used was different, the samples were cut at a different depth in the cornea, and the samples were placed in a glutaraldehyde fixative before imaging in the Serrao et al. study.

We found that the smoothest cuts were obtained at a depth of 300 μm . A previous study⁶ found that lamellar cut smoothness decreased as the cut depth increased. The posterior stroma is known to be anatomically different from the anterior stroma, which may explain why the roughness would vary as a function of depth. In addition, deeper cuts will result in more laser scatter and consequent attenuation of laser energy. In the current study, corneal hydration was brought back to physiologic levels through the use of 25% dextran. This preparation protocol was effective at removing the water taken up in the cornea postmortem for the 200 μm and 400 μm cut depths. The deeper cut was rougher than the more superficial cut, which corresponds to data available in the literature.⁶ However, the longer postmortem time of the 300 μm cut depth made the preparation protocol less effective at restoring the cornea to physiologic levels. The differences in the hydration state of this pair of eyes could have affected the results obtained in this study. This observation stresses the importance of proper maintenance of hydration during experimentation. In addition, our analysis of the effect of cut depth within the energy levels is confounded by with the donor from whom the eyes came. The low-energy versus high-energy analysis was performed on paired eyes; however, the analysis as a function of cut depth was on eyes from different

individuals. It is possible that the 300 μm cuts were smoother due to intrinsic characteristics of that particular individual's cornea.

During the imaging, the corneas were hydrated with a balanced salt solution, which can result in corneal swelling over time. In addition, 4 slits were made in the cornea so that it would lie flat on the glass slide. These slits served as an additional entry point for the balanced salt solution during the 3 hours it took to acquire the images. To address these hydration concerns during lengthy AFM imaging, previous researchers^{13,15,19} fixed the cornea in 2.5% glutaraldehyde 24 hours before imaging. Dehydrating the samples will eliminate swelling during imaging. However, we wanted to acquire images and perform roughness analysis of fresh unfixed samples. To determine whether changes in hydration affected the quantitative roughness calculated, we analyzed the roughness parameters as a function of time and found no significant relationship. We are therefore confident that any differences in roughness observed were due to the cut and not to sample hydration.

Previous studies of the cornea ultrastructure using AFM were performed in contact mode^{13,14,20,21} and tapping mode.²²⁻²⁷ Although contact mode produces lateral drag forces that may damage the sample, it was selected for this study because the lateral forces present on compliant samples during tapping mode will likely blur the surface features important in the roughness analysis. Sample damage was most likely minimized by the low contact force that was maintained throughout the imaging. Qualitatively, the images obtained in the current study are comparable to those available in the literature.¹³

Atomic force microscopy was used to provide quantitative information on the quality of lamellar dissections at different depths and energy settings using the Visumax femtosecond laser. Additional studies using AFM should be performed to compare the cut quality using different femtosecond lasers. This information may be useful to optimize patient outcomes in refractive and lamellar keratoplasty surgeries.

Acknowledgments

Supported by Carl Zeiss Meditec AG, Dublin, California, Florida Lions Eye Bank, Miami, Florida, National Institutes of Health, Bethesda, Maryland (center grant P30-EY014801 and IMSD [J.D.] and F31-EY-21714-01 [J.D.]), Research to Prevent Blindness, New York, New York, National Science Foundation, Arlington, Virginia, USA (MRI 0722372 [Dr. Moy]), an Instrumentation Grant from the James and Esther King Program, Florida Department of Health, Tallahassee, Florida (Dr. Moy).

REFERENCES

1. Yoo SH, Kymionis GD, Koreishi A, Ide T, Goldman D, Karp CL, O'Brien TP, Culbertson WW, Alfonso EC. Femtosecond laser-assisted sutureless anterior lamellar keratoplasty. *Ophthalmology*. 2008; 115:1303–1307. [PubMed: 18171586]
2. Jones YJ, Goins KM, Sutphin JE, Mullins R, Skeie JM. Comparison of the femtosecond laser (IntraLase) versus manual microkeratome (Moria ALTK) in dissection of the donor in endothelial keratoplasty; initial study in eye bank eyes. *Cornea*. 2008; 27:88–93. [PubMed: 18245973]
3. Monterosso C, Fasolo A, Caretti L, Monterosso G, Buratto L, Böhm E. Sixty-kilohertz femtosecond laser-assisted endothelial keratoplasty: clinical results and stromal bed quality evaluation. *Cornea*. 2011; 30:189–193. [PubMed: 20885308]
4. Mootha VV, Heck E, Verity SM, Petroll WM, Lakshman N, Muftuoglu O, Bowman RW, McCulley JP, Cavanagh HD. Comparative study of Descemet stripping automated endothelial keratoplasty donor preparation by Moria CBm microkeratome, Horizon microkeratome, and IntraLase FS60. *Cornea*. 2011; 30:320–324. [PubMed: 21304290]
5. Malta JB, Soong HK, Shtein R, Banitt M, Musch DC, Sugar A, Mian SI. Femtosecond laser-assisted keratoplasty: laboratory studies in eye bank eyes. *Curr Eye Res*. 2009; 34:18–25. [PubMed: 19172466]

6. Soong HK, Mian S, Abbasi O, Juhasz T. Femtosecond laser-assisted posterior lamellar keratoplasty; initial studies of surgical technique in eye bank eyes. *Ophthalmology*. 2005; 112:44–49. [PubMed: 15629819]
7. Terry MA, Ousley PJ, Will B. A practical femtosecond laser procedure for DLEK endothelial transplantation; cadaver eye histology and topography. *Cornea*. 2005; 24:453–459. [PubMed: 15829805]
8. Sarayba MA, Ignacio TS, Binder PS, Tran DB. Comparative study of stromal bed quality by using mechanical, IntraLase femtosecond laser 15- and 30-kHz microkeratomes. *Cornea*. 2007; 26:446–451. [PubMed: 17457194]
9. Sarayba MA, Ignacio TS, Tran DB, Binder PS. A 60 kHz IntraLase femtosecond laser creates a smoother LASIK stromal bed surface compared to a Zyoptix XP mechanical microkeratome in human donor eyes. *J Refract Surg*. 2007; 23:331–337. [PubMed: 17455827]
10. Sarayba MA, Maguen E, Salz J, Rabinowitz Y, Ignacio TS. Femtosecond laser keratome creation of partial thickness donor corneal buttons for lamellar keratoplasty. *J Refract Surg*. 2007; 23:58–65. [PubMed: 17269245]
11. Kermani O, Oberheide U. Comparative micromorphologic in vitro porcine study of IntraLase and Femto LDV femtosecond lasers. *J Cataract Refract Surg*. 2008; 34:1393–1399. [PubMed: 18655994]
12. Cheng YYY, Kang SJ, Grossniklaus HE, Pels E, Duimel HJQ, Frederik PM, Hendrikse F, Nuijts RMMA. Histologic evaluation of human posterior lamellar discs for femtosecond laser Descemet's stripping endothelial keratoplasty. *Cornea*. 2009; 28:73–79. [PubMed: 19092410]
13. Lombardo M, De Santo MP, Lombardo G, Barberi R, Serrao S. Atomic force microscopy analysis of normal and photoablated porcine corneas. *J Biomech*. 2006; 39:2719–2724. Available at: <http://www.visioeng.it/documents/AFMJBioMechanics.pdf>. [PubMed: 16209868]
14. Nógrádi A, Hopp B, Révész K, Szabó G, Bor Z, Kolozsvári L. Atomic force microscopic study of the human cornea following excimer laser keratectomy. *Exp Eye Res*. 2000; 70:363–368. [PubMed: 10712822]
15. Serrao S, Lombardo M, De Santo MP, Lombardo G, Schiano Lomoriello D, Ducoli P, Stirpe M. Femtosecond laser photodisruptive effects on the posterior human corneal stroma investigated with atomic force microscopy. *Eur J Ophthalmol*. 2012; 22(suppl 7):S89–S97. [PubMed: 22267457]
16. Binnig G, Quate CF, Gerber C. Atomic force microscope. *Phys Rev Lett*. 1986; 56:930–933. [PubMed: 10033323]
17. Tomanek D, Overney G, Miyazaki H, Mahanti SD, Guntherodt HJ. Theory for the atomic force microscopy of deformable surfaces. *Phys Rev Lett*. 1989; 63:876–879. [PubMed: 10041208]
18. Borja D, Manns F, Lamar P, Rosen A, Fernandez V, Parel J-M. Preparation and hydration control of corneal tissue strips for experimental use. *Cornea*. 2004; 23:61–66. [PubMed: 14701959]
19. Lombardo M, De Santo MP, Lombardo G, Schiano Lomoriello D, Desiderio G, Ducoli P, Barberi R, Serrao S. Surface quality of femtosecond dissected posterior human corneal stroma investigated with atomic force microscopy. *Cornea*. May 29, 2012 Epub ahead of print.
20. Fullwood NJ, Hammiche A, Pollock HM, Hourston DJ, Song M. Atomic force microscopy of the cornea and sclera. *Curr Eye Res*. 1995; 14:529–535. [PubMed: 7587298]
21. Meller D, Peters K, Meller K. Human cornea and sclera studied by atomic force microscopy. *Cell Tissue Res*. 1997; 288:111–118. [PubMed: 9042778]
22. Abrams GA, Schaus SS, Goodman SL, Nealey PF, Murphy CJ. Nanoscale topography of the corneal epithelial basement membrane and Descemet's membrane of the human. *Cornea*. 2000; 19:57–64. [PubMed: 10632010]
23. Last JA, Russell P, Nealey PF, Murphy CJ. The applications of atomic force microscopy to vision science. *Invest Ophthalmol Vis Sci*. 2010; 51:6083–6094. Available at: <http://www.iovs.org/content/51/12/6083.full.pdf>.
24. Yamamoto S, Hitomi J, Sawaguchi S, Abe H, Shigeno M, Ushiki T. Observation of human corneal and scleral collagen fibrils by atomic force microscopy. *Jpn J Ophthalmol*. 2002; 46:496–501. Available at: <http://www.nichigan.or.jp/jjo-oj/pdf/04605/046050496.pdf>. [PubMed: 12457907]

25. Yamamoto S, Hashizume H, Hitomi J, Shigeno M, Sawaguchi S, Abe H, Ushiki T. The subfibrillar arrangement of corneal and scleral collagen fibrils as revealed by scanning electron and atomic force microscopy. *Arch Histol Cytol.* 2000; 63:127–135. Available at: https://www.jstage.jst.go.jp/article/aohc/63/2/63_2_127/_pdf. [PubMed: 10885449]
26. Yamamoto S, Hitomi J, Sawaguchi S, Abe H, Shigeno M, Ushiki T. Observation of human corneal and scleral collagen fibrils by atomic force microscopy]. [Japanese] *Nippon Ganka Gakkai Zasshi.* 1999; 103:800–805. English abstract available in *Jpn J Ophthalmol* 2000; 44:318. [PubMed: 10589238]
27. Yamamoto S, Hitomi J, Shigeno M, Sawaguchi S, Abe H, Ushiki T. Atomic force microscopic studies of isolated collagen fibrils of the bovine cornea and sclera. *Arch Histol Cytol.* 1997; 60:371–378. [PubMed: 9412740]

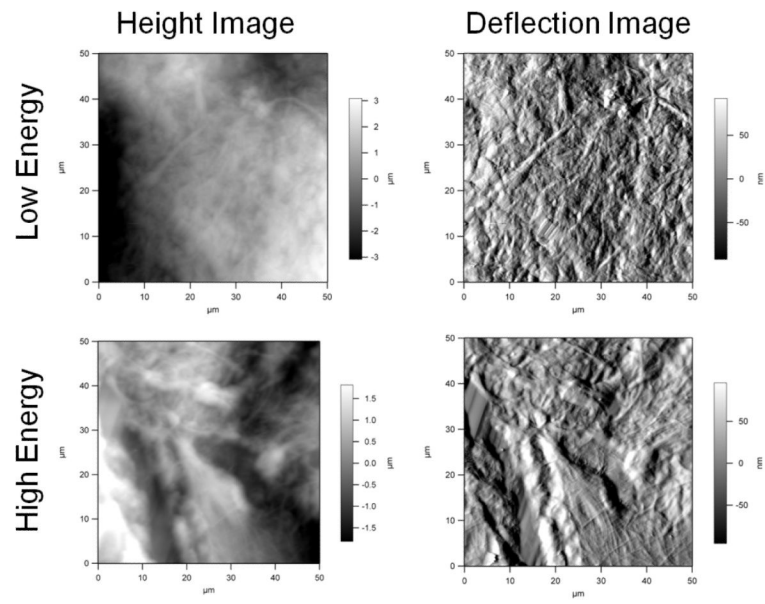


Figure 1.
Atomic force microscopy images of the 200 μm cut depth.

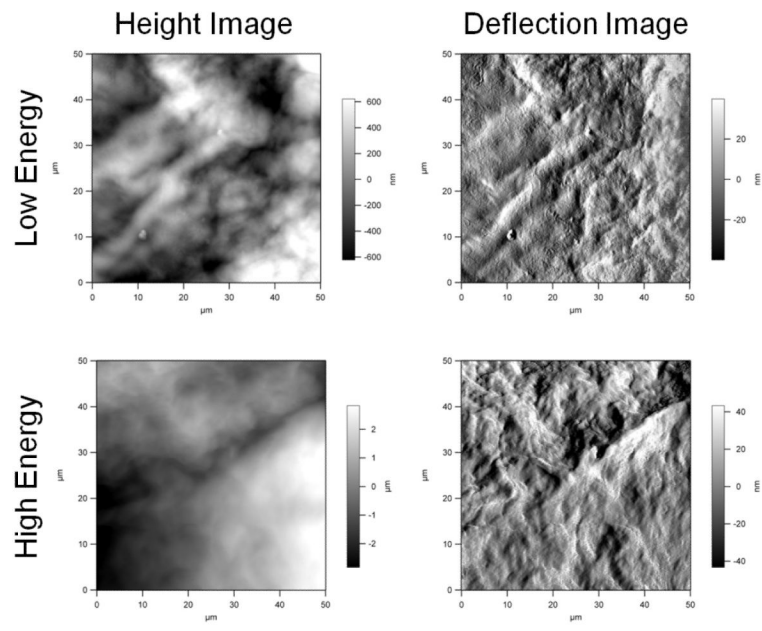


Figure 2.
Atomic force microscopy images of the 300 μm cut depth.

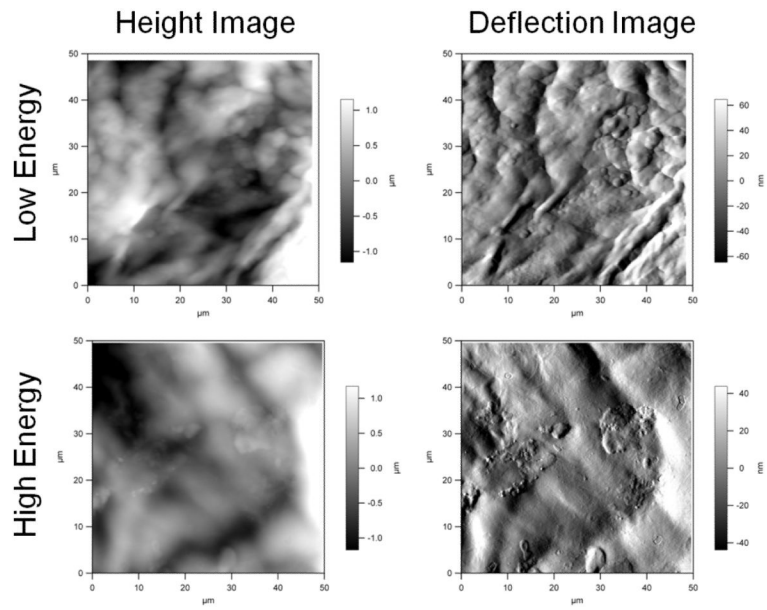


Figure 3.
Atomic force microscopy images of the 400 μm cut depth.

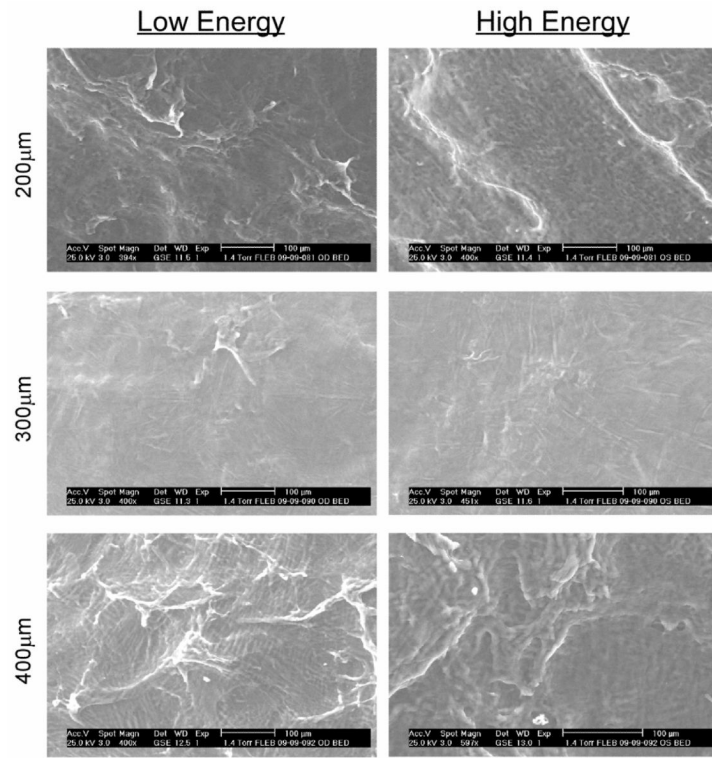


Figure 4. Environmental SEM images obtained on the posterior face of the lamellar incision of same samples used for the AFM imaging studies.

Table 1

Donor information for the 2 pairs of eyes used in this study. The cornea thickness measurements were obtained using OCT.

Pair	Age (Y)	Postmortem Time (D)	Laser Settings		
			Cornea Thickness (μm)	Cut Energy (nJ)	Cut Depth (μm)
1	84	3			
	RE	—	478	180	200
	LE	—	433	340	200
2	68	6			
	RE	—	637	180	300
	LE	—	950	340	300
3	84	3			
	RE	—	516	180	400
	LE	—	575	340	400

Table 2

Summary of roughness parameters for the 200 mm, 300 mm, and 400 mm depths.

Cut Depth/Energy	Mean \pm SD*			
	RMS Deviation (mm)	Average Deviation (mm)	Skewness	Kurtosis
200 μ m				
Low	0.93 \pm 0.73	0.86 \pm 0.57	-0.10 \pm 0.35	-0.48 \pm 0.42
High	1.03 \pm 0.67	0.87 \pm 0.59	0.04 \pm 0.19	-0.57 \pm 0.46
300 μ m				
Low	0.41 \pm 0.26	0.33 \pm 0.21	0.11 \pm 0.41	-0.05 \pm 0.27
High	1.44 \pm 0.04	1.17 \pm 0.08	-0.17 \pm 0.39	-0.35 \pm 0.71
400 μ m				
Low	0.83 \pm 0.33	0.64 \pm 0.26	0.49 \pm 0.64	0.73 \pm 0.96
High	0.74 \pm 0.57	0.60 \pm 0.48	-0.30 \pm 0.73	0.36 \pm 1.51

RMS = root mean square

* Of all images included in analysis